

Stability analysis on dual solutions of second- grade fluid flow with heat and mass transfers over a stretching sheet

Debasish Dey, Rupjyoti Borah *

Department of Mathematics, Dibrugarh University, Dibrugarh-786004, Assam, India

Received: 05 January 2021; Received in revised form: 18 March 2021; Accepted: 20 April 2021;
Published online 28 April 2021

© Published at www.ijtf.org

Abstract

Stability on dual solutions of second-grade fluid flow over a stretching surface with simultaneous thermal and mass diffusions has been studied. The fluid flow is governed by Lorentz force and energy dissipation due to viscosity. Lorentz force is generated due to the application of magnetic field along the transverse direction. In methodology, suitable similarity transformation and MATLAB built-in `bvp4c` solver technique have been adopted. Effects of some flow parameters are exhibited through figures and tables and a special emphasis is given on the existence of dual solutions. A stability analysis is executed to determine the stable and physically achievable solutions. For the laminar flow, the drag force on the surface for the time-independent case is reduced due to amplifying values of Re . But, it enhances the drag force for the time-dependent case. This shows the effectiveness of the first solution (during steady case) over the unsteady case.

Keywords: Dual solutions, heat transfer, mass transfer, stability analysis, stretching sheet, visco-elastic fluid.

1. Introduction

Fluid flow over the extending/shrinking surface has attracted many researcher attentions due to its wide range of applications in industrial purpose. The study of fluid flow due to extending geometries can be related to polymer extrusion, drawing or plastic films, hot rolling, casting etc. Crane [1] was the first author who introduced the flow problem over a linearly stretching sheet. Again, the fluid flow in presence of a magnetic field is very important in applied sciences, engineering and industrial processes such as MHD pumps and MHD power generator etc. Many researchers have taken the magnetic field for controlling fluid and enhancing temperature of the system. Makinde *et al.*[2], Farooq *et al.* [3] and Krishna *et al.*[4] have investigated the effects of magnetic field on fluid flows over various stretching surfaces.

The viscoelastic fluid is a special kind of non-Newtonian fluid having both viscous and elastic properties. The momentum, thermal and mass transfer phenomena in a viscoelastic boundary layer have been investigated widely in the modern time because of their applications in the polymer processing industries and other physical fields. The recent advancement of modern technologies has triggered many researchers to study the fluid flows with simultaneous effects of both thermal and mass transfer and other interactive physical phenomena.

Nomenclature			
A	constant	u	velocity along x – direction, m/s
B	constant	v	velocity along y – direction, m/s
B_0	strength of magnetic field, A/m	<i>Greek Symbols</i>	
C	concentration of the fluid, mol/m ³	μ	dynamic viscosity, kg/m s
C_f	skin friction coefficient	ν	kinematic viscosity, m ² /s
C_p	specific heat at constant pressure, J/kg K	ω	eigen-value parameter
c	shrinking/stretching constant	$\phi(\eta)$	dimensionless fluid concentration
D_m	mass diffusivity, m ² /s	ρ	density of the fluid, kg/m ³
Ec	Eckert number	σ	electric conductivity
$f'(\eta)$	dimensionless fluid velocity	ψ	stream function
K	fluid thermal conductivity, W/m K	τ	dimensionless time variable
k	visco-elastic parameter	τ_w	shear stress
M	magnetic parameter	$\theta(\eta)$	dimensionless fluid temperature
Nu_x	local Nusselt number	<i>Subscripts</i>	
Pr	Prandtl number	w	at wall
q_w	heat flux	∞	at ambient situation
Re_x	local Reynold number	<i>Superscript</i>	
Sc	Schmidt number	'	prime (differentiation with respect to the dimensionless variable η)
T	temperature of the fluid, K		
t	time, s		

Again, there are multifarious applications of both thermal and mass transfers in stretching/shrinking surfaces such as annealing and thickening of copper wire etc. Turkyilmazoglu [5] has studied the simultaneous effects of thermal and concentration on the boundary layer flow using analytical technique. Othman *et al.*[6] have investigated the boundary layer flow of nanofluid due to stretching/shrinking surface and interpreted the importance appliance of thermal and mass transfer effects on different physical fields. Anwar *et al.*[7] have examined the flow behaviour of non-Newtonian fluid due to stretching type surface by adopting numerical scheme. Asghar *et al.*[8] have investigated the steady three dimensional flow of viscous fluid with thermal effect due to rotating disk which is stretched in radial direction. Many authors, (Alharbi *et al.* [9], Ghadikolaie *et al.* [10], Salah and Elhafian [11], Dey [12, 13]) have investigated the boundary layer flow with heat and mass transfers of visco-elastic fluid over different geometries. Very recently, Shankar Goud [14] has studied the influence of thermal radiation and magnetic field on the boundary layer flow caused by stretching surface. Hayat *et al.*[15] have studied the simultaneous effects of thermal and mass transfer phenomena on the boundary layer flow between two parallel disks using visco-elastic fluid model. Sailaja *et al.*[16] have developed the importance of natural and forced convection heat transfer of the nanofluid which is caused by vertical stretching surface and put their importance on the different physical fields such as engineering sciences, medical sciences and other industrial processes etc.

Due to stretching/shrinking type surfaces, a sudden change (disturbances) of the flow nature is noticed during the fluid flow. Initially, there may not be any disturbances on the flow when the surface is at rest. For that situation, the boundary layer flow provides steady type solution which is tractable in practice. But, when the surface is going to stretch or shrink, an initial growth of

disturbances is observed on the flow which affects the flow behaviour and both thermal and mass transfer phenomena are dependent on time. In this situation, a new branch of solution which is dependent on time is developed. Markin [17] was the first author who developed the dual type (lower branch and upper branch) solutions for the boundary layer flow and given their important physical significance. Othman *et al.* [6] have investigated the dual solutions of nanofluid flow due to shrinking surface and established that the time-independent solutions is physically tractable. Turkyilmazoglu [18] has studied multiple solutions of boundary layer flow of present fluid model by analytical technique. Recently, many researchers (Zaimi *et al.* [19], Naramgari *et al.* [20], Anuar *et al.* [21] and Dey and Borah [22] etc) have investigated the dual solutions of different fluid models and their stability of the boundary layer flow over different expanding/contracting surfaces. They have established that first solution is stable and physically achievable.

The main intention of this study is to investigate the behaviour of dual solutions due to boundary layer flow of second-grade fluid with thermal and mass transmissions over an expanding sheet in presence of uniform magnetic field. The governing partial differential equations are transformed into a set of ordinary differential equations using appropriate similarity transformations and have been solved numerically by MATLAB built-in bvp4c solver technique. A comparison of our work has been made with the results of Ghadikolaie *et al.* [10]. We have extended the work of [10] by considering the effects of magnetic field and the mass diffusion on the visco-elastic fluid flow and their multiple solutions that occurred due to stretching type surface Different novel flow parameters involved in this problem are interpreted in the physical sense.

2. Formulation of the problem

The two-dimensional, steady, laminar and incompressible boundary layer flow past a stretching surface with heat and mass transfers of non-Newtonian second-grade fluid has been considered. The flow model and coordinate system is shown by figure (1). The sheet behaves like an elastic surface i.e., two equal and opposite forces are applied along x-direction of the sheet for which sheet is stretched and reserved and the origin fixed. A uniform magnetic field B_0 is applied along the normal direction of the flow. Using boundary layer approximations, the governing equations of fluid motion are (following Ghadikolaie *et al.* [10]):

$$\frac{\partial u}{\partial x} + \frac{\partial v}{\partial y} = 0, \quad (1)$$

$$u \frac{\partial u}{\partial x} + v \frac{\partial u}{\partial y} = \nu \frac{\partial^2 u}{\partial y^2} + \frac{\alpha_1}{\rho} \left[\frac{\partial}{\partial x} \left(u \frac{\partial^2 u}{\partial y^2} \right) + \frac{\partial u}{\partial y} \frac{\partial^2 v}{\partial y^2} + v \frac{\partial^3 u}{\partial y^3} \right] - \frac{\sigma B_0^2}{\rho} u, \quad (2)$$

$$u \frac{\partial T}{\partial x} + v \frac{\partial T}{\partial y} = \alpha \frac{\partial^2 T}{\partial y^2} + \frac{K}{\rho C_p} \left(\frac{\partial u}{\partial y} \right)^2, \quad (3)$$

$$u \frac{\partial C}{\partial x} + v \frac{\partial C}{\partial y} = D_m \frac{\partial^2 C}{\partial y^2}. \quad (4)$$

The associated boundary conditions are (following Ghadikolaie *et al.* [10]):

$$u = u_w = cx, v = 0, T = T_w (= T_\infty + Ax^s), C = C_w (= C_\infty + Bx) : y = 0, \\ u \rightarrow 0, \frac{\partial u}{\partial y} \rightarrow 0, T \rightarrow T_\infty, C \rightarrow C_\infty : y \rightarrow \infty, \quad (5)$$

where, $u_w, T_w, T_\infty, C_w, C_\infty, s$ & (A, B) are wall velocity, wall temperature, free stream temperature, wall concentration, ambient concentration, wall temperature parameter and constants respectively. The constant $c > 0$ signifies stretch at the surface.

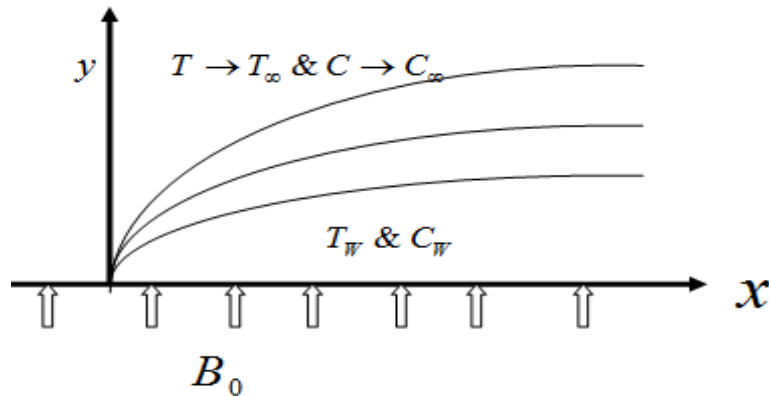


Fig. 1 Flow model and coordinate system

The following similarity transformations are introduced to renovate the above governing equations into a set of ordinary differential equations.

$$\psi = \sqrt{c\nu}xf(\eta), \eta = \sqrt{\frac{c}{\nu}}y, \theta(\eta) = \frac{T-T_\infty}{T_w-T_\infty}, \phi(\eta) = \frac{C-C_\infty}{C_w-C_\infty}, \quad (6)$$

where, ψ is the stream function such that the velocity components can be derived as $u = \frac{\partial\psi}{\partial y}$ &

$v = -\frac{\partial\psi}{\partial x}$. Therefore, we have obtained the following set of ordinary differential equations:

$$f''^2 - ff'' = f'''' + k[2f'f''' - f''^2 - ff^{iv}] - Mf', \quad (7)$$

$$\theta'' + Pr f\theta' - sPr f'\theta = -Pr Ec f''^2, \quad (8)$$

$$\phi'' + Sc f\phi' - Sc f'\phi = 0, \quad (9)$$

where, prime represents differentiation with respect to dimensionless variable η .

$M = \frac{\sigma B_0^2}{\rho c}, k = \frac{\alpha_1 c}{\rho \nu}, Pr = \frac{\nu}{\alpha}, Sc = \frac{\nu}{D_m}$ & $Ec = \frac{c^2 x^2}{AC_p x^s}$ are the magnetic parameter, visco-elastic

parameter, Prandtl number, Schmidt number and Eckert number respectively. The relevant boundary conditions are:

$$\begin{aligned} f(0) = 0, f'(0) = 1, \theta(0) = 1, \phi(0) = 1; \\ f'(\eta) \rightarrow 0, f''(\eta) \rightarrow 0, \theta(\eta) \rightarrow 0, \phi(\eta) \rightarrow 0 \text{ as } \eta \rightarrow \infty. \end{aligned} \quad (10)$$

The physical quantities of interest in many practical applications in engineering and industrial processes which are observed in this study are skin friction coefficient ($C_f = \frac{\tau_w}{\rho u_w^2}$), and Nusselt

number ($Nu_x = \frac{xq_w}{K(T_w - T_\infty)}$). Where, $\tau_w = \mu \left(\frac{\partial u}{\partial y} \right)_{y=0}$ is the shear stress, $q_w = -K \left(\frac{\partial T}{\partial y} \right)_{y=0}$ the heat

flux. Therefore, the expressions for these quantities are:

$$f''(0) = (\text{Re}_x)^{\frac{1}{2}} C_f, -\theta'(0) = (\text{Re}_x)^{-\frac{1}{2}} Nu_x, \text{ where, } \text{Re}_x = \frac{u_w x}{\nu} \text{ is the local Reynolds number.}$$

3. Stability Analysis

The stability analysis is performed to determine which solution will be more (or less) stable and realizable. Markin [17] was the first author who established the flow stability on dual solutions for the boundary-layer fluid flow of mixed convection in a porous medium. To investigate this nature of this fluid flow, we have considered the unsteady form of these governing equations by adding $\frac{\partial u}{\partial t}, \frac{\partial T}{\partial t}$ & $\frac{\partial C}{\partial t}$ in (2 – 4) where, t denotes the time. The following similarity variables are needed to

remodel the above equations into ordinary differential equations.

$$\psi = \sqrt{c\nu}xf(\eta, \tau), \eta = \sqrt{\frac{c}{\nu}}y, \theta(\eta, \tau) = \frac{T - T_\infty}{T_w - T_\infty}, \phi(\eta, \tau) = \frac{C - C_\infty}{C_w - C_\infty}, \tau = ct. \quad (11)$$

Then we have obtained the following similarity equations:

$$\frac{\partial^2 f}{\partial \eta \partial \tau} + \left(\frac{\partial f}{\partial \eta}\right)^2 - f \frac{\partial^2 f}{\partial \eta^2} = \frac{\partial^3 f}{\partial \eta^3} + k \left[2 \frac{\partial f}{\partial \eta} \frac{\partial^3 f}{\partial \eta^3} - \left(\frac{\partial^2 f}{\partial \eta^2}\right)^2 - f \frac{\partial^4 f}{\partial \eta^4} \right] - M \frac{\partial f}{\partial \eta}, \quad (12)$$

$$\frac{\partial^2 \theta}{\partial \eta^2} + \text{Pr} f \frac{\partial \theta}{\partial \eta} - s \text{Pr} \frac{\partial f}{\partial \eta} \theta - \text{Pr} \frac{\partial \theta}{\partial \tau} + \text{Pr} Ec \left(\frac{\partial^2 f}{\partial \eta^2}\right)^2 = 0, \quad (13)$$

$$\frac{\partial^2 \phi}{\partial \eta^2} + Scf \frac{\partial \phi}{\partial \eta} - Sc \frac{\partial f}{\partial \eta} \phi - Sc \frac{\partial \phi}{\partial \tau} = 0. \quad (14)$$

The relevant boundary conditions are:

$$f(0, \tau) = 0, \frac{\partial f(0, \tau)}{\partial \eta} = 1, \theta(0, \tau) = 1, \phi(0, \tau) = 1; \quad (15)$$

$$\frac{\partial f(\infty, \tau)}{\partial \eta} \rightarrow 0, \frac{\partial^2 f(\infty, \tau)}{\partial \eta^2} \rightarrow 0, \theta(\infty, \tau) \rightarrow 0, \phi(\infty, \tau) \rightarrow 0.$$

For the check of stability, we consider the steady flow solutions $f(\eta) = f_0(\eta), \theta(\eta) = \theta_0(\eta)$ and $\phi(\eta) = \phi_0(\eta)$ which satisfy the boundary value problem (7)-(10) and can be obtained by putting $\tau = 0$. Following Markin [17] and Dey and Borah [22], we have taken the following perturb equations:

$$f(\eta, \tau) = f_0(\eta) + e^{-\omega\tau} F(\eta, \tau), \theta(\eta, \tau) = \theta_0(\eta) + e^{-\omega\tau} G(\eta, \tau), \quad (16)$$

$$\phi(\eta, \tau) = \phi_0(\eta) + e^{-\omega\tau} H(\eta, \tau),$$

where, ω is the unknown eigen-value parameter, and $F(\eta, \tau), G(\eta, \tau)$ and $H(\eta, \tau)$ are small related to the steady flow solutions. Applying equation (19) in equations (15)-(17) and then using $F(\eta) = F_0(\eta), G(\eta) = G_0(\eta)$ and $H(\eta) = H_0(\eta)$, then we have got the following set of eigen value problem:

$$F_0'''' + k \left[2(f_0' F_0'''' + F_0' f_0'''') - 2f_0'' F_0'' - f_0 F_0'''' - F_0 f_0'''' \right] - M F_0' - 2f_0' F_0' + f_0 F_0'' \quad (17)$$

$$+ F_0 f_0'' + \omega F_0' = 0,$$

$$G_0'' + \text{Pr} (f_0' G_0' + F_0 \theta_0') - s \text{Pr} (f_0' G_0 + F_0' \theta_0) + \omega \text{Pr} G_0 + 2 \text{Pr} Ec f_0'' F_0'' = 0, \quad (18)$$

$$H_0'' + Sc(f_0 H_0' + F_0 \phi_0') - Sc(f_0' H_0 + F_0' \phi_0) + \omega Sc H_0 = 0, \quad (19)$$

the boundary conditions are:

$$\begin{aligned} F_0(0) = 0, F_0'(0) = 0, G_0(0) = 0, H_0(0) = 0; \\ F_0'(\infty) \rightarrow 0, F_0''(\infty) \rightarrow 0, G_0(\infty) \rightarrow 0, H_0(\infty) \rightarrow 0. \end{aligned} \quad (20)$$

For particular values of flow parameters, the corresponding stability of the steady flow solutions $f(\eta) = f_0(\eta)$, $\theta(\eta) = \theta_0(\eta)$ and $\phi(\eta) = \phi_0(\eta)$ are obtained by smallest eigen values ω and F_0, G_0 and H_0 recognize the initial disturbance of equation (19). The smallest positive eigen value recognizes stable flow. Following Harish *et al.* [23], the boundary condition $F_0'(\infty) \rightarrow 0$ is reduced to $F_0''(0) = 1$ for getting achievable eigen-values.

4. Methodology

Following Dey and Hazarika [24] and Dey and Chutia [25], the ‘‘MATLAB routine bvp4c solver scheme’’ is adopted to solve the equations [(7)-(9)] and [(17)-(19)] with their respective boundary conditions (10) and (20). It works out the results numerically by taking finite difference codes and resolving the error indirectly. The users have to put their system of equations into a new system by launching new variables as the following:

$$f = d_1, f' = d_2, f'' = d_3, f''' = d_4, \theta = d_5, \theta' = d_6, \phi = d_7 \text{ \& } \phi' = d_8.$$

So, we have achieved first order equations of system:

$$\begin{aligned} d_4' &= \frac{k(2d_2d_4 - d_3^2) - (d_2^2 - d_1d_3 + Md_2 - d_4)}{kd_1}, d_1' = d_2, d_2' = d_3 \\ , d_3' &= d_4; d_5' = d_6, d_6' = \text{Pr}(sd_2d_5 - Ecd_3^2 - d_1d_6); d_7' = d_8, \\ d_8' &= Sc(d_2d_7 - d_1d_8). \end{aligned}$$

The relevant boundary conditions take the following form:

$$d0(1), d0(2) - 1, d0(5) - 1, d0(7) - 1; d1(2), d1(3), d1(5), d1(7).$$

4. Results and Discussion

In this investigation, we have denoted the first solution (during steady case) as solid line and the second solution which is responsible for time-dependent solution as dotted line. A special stress is given on nature of dual solutions with different involving flow parameters of this problem.

The figures (2) and (3) are prepared to illustrate the effects of Hartmann number (M) on the velocity and temperature of the fluid motion with $\text{Pr}=13.4$ (sea water), $\text{Sc}=0.61$ and $k=0.22$. It is seen in Fig. 2 that the magnetic parameter ‘M’ reduces the velocity of fluid flow during time free case, but it enhances the speed of the fluid during time dependent case (second solution). Physically, it can be attributed that the transverse magnetic field on the electrically conducting fluid motion generates a resistive type force called ‘‘Lorentz force’’ and consequently fluid’s motion reduces. Further, the first solution clearly shows more stability over the second solution. Also, the width of the momentum boundary layer for first solution (during steady case) is lesser than the second solution (during unsteady case). The strong magnetic field (enhancing values of M) elevates the temperature of the fluid flow (during time independent case) until thermal equilibrium stage is reached (Fig. 3). Thus, we can conclude that for enhancing the temperature of a system, the Lorentz force plays a major role. On

the other hand, the second solution, dependent on time, shows an opposite nature with the first solution.

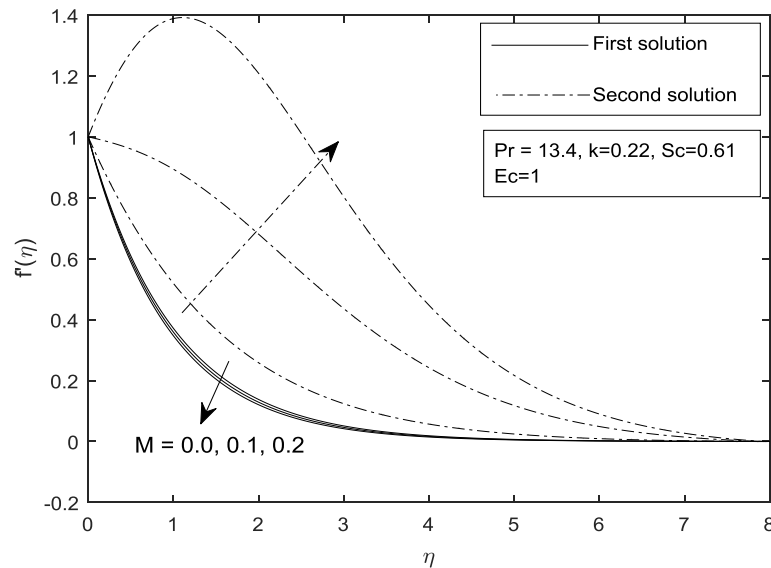


Fig.2 Velocity profile $f'(\eta)$ against η for incremental values of magnetic parameter (M).

The visco-elasticity of fluid flow is exhibited by the parameter (k) and its effects on flow characteristics are shown by Figs. 4 and 5 with fixed values of Pr, Sc and $M=0.2$. The smaller values of k characterizes smaller deformation rate. The figure 4 tells that first solution experiences acceleration due to 'k'. But a reverse trend is noticed in time-dependent solution (second solution). Geometrically, we can interpret that the time-independent solution reaches its free stream region more sooner than time-dependent solutions. This shows that stability of first solution over second solution. In the figure 5, we have represented temperature profile against displacement variable for various values of k for the sea-water ($Pr = 13.4$). Dual nature of temperature profile is seen during the growth of the visco-elastic parameter (k).

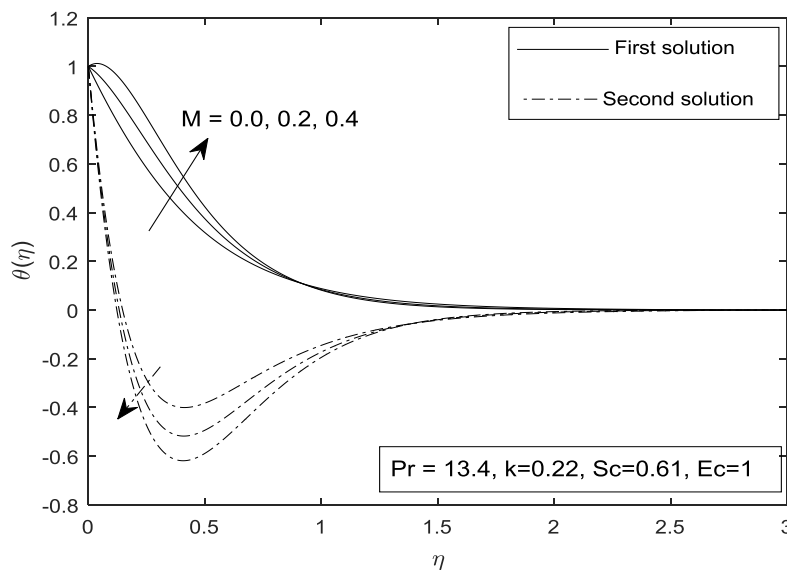


Fig. 3 Temperature Profile $\theta(\eta)$ against η for incremental values of magnetic parameter (M).

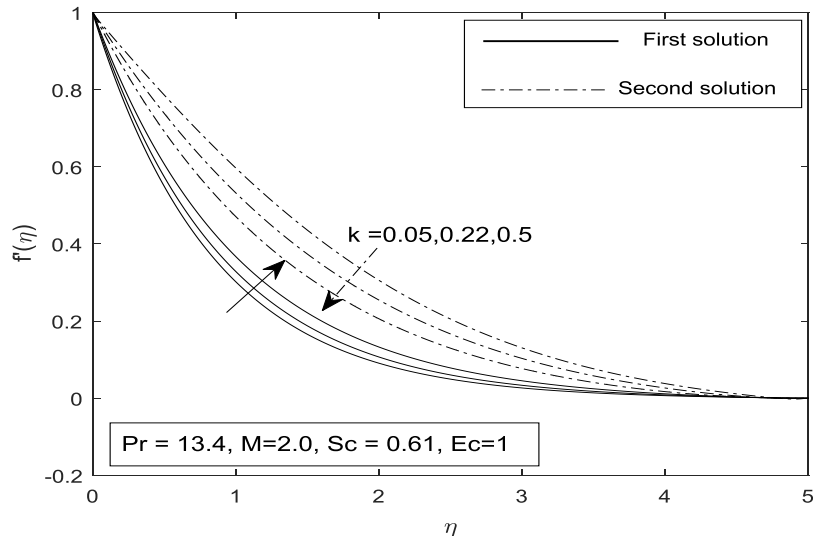


Fig. 4 Velocity profile $f'(\eta)$ against η for incremental values of visco-elastic parameter (k).

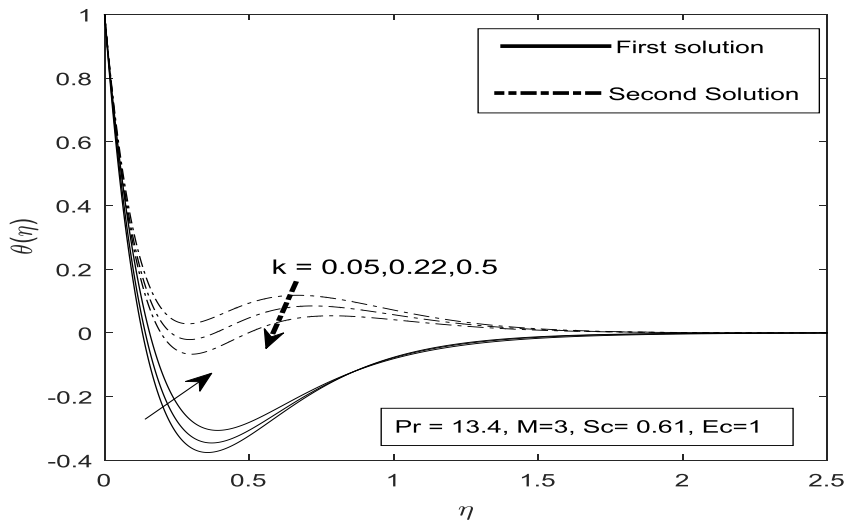


Fig.5 Temperature $\theta(\eta)$ profiles against η for various values of visco-elastic parameter (k).

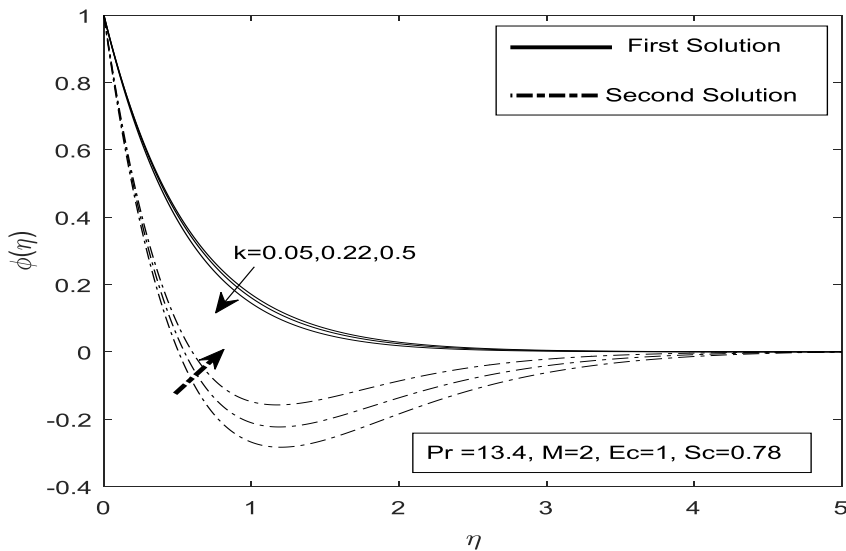


Fig. 6 Concentration $\phi(\eta)$ profiles for various values of visco-elastic parameter (k).

Temperature grows up with the variation of k is seen during steady flow solution (first solution) but its reverse nature is seen during unsteady flow solution (second solution) until thermal equilibrium stage is reached. Similarly, figure (6) also reveals that the visco-elastic parameter (k) subdues the mass deposition of the first solution but mass deposition is enhanced during unsteady flow (second solution). Thus, the visco-elasticity plays an important role in developing the dual natures.

We have compared our numerical values of first solution of heat transfer rate at the surface of the sheet (Nusselt number) with previously published paper by Ghadikolaie *et al.* [10] to demonstrate the truth of our results and hence it shows a good conformity. It is also observed from table (1) that the magnitudes of the first and second solutions increase as the increasing values of visco-elastic parameter (k).

TABLE.1 Numerical values Nusselt number ($-\theta'(0)$) for various values of visco-elastic parameter (k) when $M=0, Sc=0, Pr=1$ & $s=2$.

Value of 'k'	η	$-\theta'(0)$ (Ghadikolaie <i>et al.</i> [10])	$-\theta'(0)$ (Present Results)	
			First solution	Second solution
0.01	0	1.334722	1.3278	2.1776
	0.1	1.150370	1.1627	2.0481
	0.2	0.993877	0.9963	1.5048
0.05	0	1.340277	1.3393	2.1844
	0.1	1.155672	1.1738	2.0540
	0.2	0.998583	0.9953	1.5069

TABLE.2 Numerical values of physical quantities for various values of the Prandtl and Schmidt numbers when $M = 2, k = 0.01, Ec = 1$.

Pr	Sc	$-\theta'(0)$		$-\phi'(0)$	
		First solution	Second solution	First solution	Second solution
0.015	0.22	0.2283	0.2466	0.3485	0.5292
7		6.6394	6.4958	0.3500	0.5383
13.5		10.3859	9.2818	0.3501	0.5389
13.4	0.22	10.6339	9.6064	0.3485	0.5292
	0.30	10.6355	9.4763	0.4001	0.6522
	0.60	10.6356	9.4674	0.5959	1.0942

From the table (2), it is perceived that the values of Nusselt number and Sherwood number for both the solutions enhance from the noble gas ($Pr = 0.015$) to sea-water ($Pr = 13.4$). In the same way, The values of mass accumulation rate ($-\phi'(0)$) boosts up during both the cases from the hydrogen ($Sc = 0.22$) to water vapour ($Sc = 0.60$). But, it reduces the second solution of the Nusselt number. The table (3) shows the nature of flow stability and it is observed that the smallest positive eigen-values recognize an initial decay of disturbances on the flow and hence the flow will be stable and the smallest negative eigen-value characterizes an initial growth of complexity on the flow which give unstable flow. From this study, we have concluded that the first solution i.e., the solution occurred

during steady flow case is stable and the second solution which is dependent on time is unstable and not physically achievable.

TABLE.3 Numerical values of smallest eigen-value ω when $M = 0.5$ & $Pr = 0.71$ for various values of k .

Visco-elastic parameter (k)	Smallest eigen- value (ω)	
	First solution	Second solution
0.2	0.1398	-0.0559
0.6	0.0224	-0.0221
0.8	0.0222	-0.0220

The Reynolds number (Re) has a vital role in the fluid dynamics because it helps to predict the flow pattern in different fluid flow situations. Again, a low Reynolds number indicates laminar flow and a high Reynolds number gives turbulent (unstable) flow. The following table-4 is established for the effects of Reynolds number in the skin friction coefficient. For the laminar flow i.e., $Re < 2000$, the skin friction coefficient for the time-independent solution (first solution) reduces and an opposite trend is noticed during second solution. For turbulent flow i.e., $Re > 4000$, only time-dependent solution (second solution) varies and enhances with Re but, the numerical values of the first solution remain constant.

TABLE-4. Numerical values of skin friction coefficient (C_f) for various values the Reynolds number (Re) when the other flow parameters are fixed.

Reynolds number (Re)	Skin friction coefficient (C_f)	
	First solution	Second solution
10	-0.0384	-0.0132
10^2	-0.0385	-0.0118
10^3	-0.0386	-0.0112
4200	-0.0172	-0.0059
4500	-0.0172	-0.0053
5000	-0.0172	-0.0050

5. Conclusion

We have seen that the dual solutions (first and second solutions) exist up to a certain region of the dimensionless variable η ($0 < \eta < 5$) for various values of flow parameters. All the profiles satisfy the far field boundary conditions asymptotically and exhibit dual nature solutions. From the stability point of view, the first solution is stable and physically achievable. The following conclusions are made from this study:

- The visco-elastic parameter helps to enhance the motion and temperature of the fluid during steady case. But, it lessens the mass deposition of the fluid during steady case.

- During steady case (first solution), the magnetic parameter plays an important role to normalize the motion of the fluid. But, it helps to raise the temperature of the system. In case of time dependent solution, it acts on the flow as opposite manner with steady case.
- For the laminar flow ($Re < 2000$), the drag force on the surface for time-independent case is reduced due to amplifying values of Re . But, it enhances the drag force for the time-dependent case. So, the first solution (during steady case) is more effective than the unsteady case.

References

- [1] L. J. Crane, Flow past a stretching plate, *Zeitschrift für Angew. Math. und Phys. ZAMP*, 21 (1970) 645–647.
- [2] O. D. Makinde, W. A. Khan, Z. H. Khan, Stagnation point flow of MHD chemically reacting nanofluid over a stretching convective surface with slip and radiative heat, *Proc. Inst. Mech. Eng. Part E J. Process Mech. Eng.*, 231(2017) 695–703.
- [3] U. Farooq, D. Lu, S. Munir, M. Ramzan, M. Suleman, S. Hussain, MHD flow of Maxwell fluid with nanomaterials due to an exponentially stretching surface, *Sci. Rep.*, 9 (2019) 1–11.
- [4] Y. H. Krishna, G. V. R. Reddy, O. D. Makinde, Chemical reaction effect on MHD flow of casson fluid with porous stretching sheet, *Defect Diffus. Forum*, 389 (2018) 100–109.
- [5] M. Turkyilmazoglu, Stretching/shrinking longitudinal fins of rectangular profile and heat transfer, *Energy Convers. Manag.*, 91 (2015) 199–203.
- [6] N. A. Othman, N. A. Yacob, N. Bachok, A. Ishak, I. Pop, Mixed convection boundary-layer stagnation point flow past a vertical stretching/shrinking surface in a nanofluid, *Appl. Therm. Eng.*, 115 (2017) 1412–1417.
- [7] M. I. Anwar, S. Shafie, T. Hayat, S. A. Shehzad, M. Z. Salleh, Numerical study for MHD stagnation-point flow of a micropolar nanofluid towards a stretching sheet, *J. Brazilian Soc. Mech. Sci. Eng.*, 39 (2017) 89–100.
- [8] S. Asghar, M. Jalil, M. Hussan, M. Turkyilmazoglu, Lie group analysis of flow and heat transfer over a stretching rotating disk, *Int. J. Heat Mass Transf.*, 69 (2014) 140–146.
- [9] S.M. Alharbi, A.A.M. Bazid, M. Elgendy, Heat and Mass transfer in MHD visco-elastic fluid flow through a porous medium over stretching sheet with chemical reaction, *Applied Mathematics*, 1 (2010) 445-446.
- [10] S. S. Ghadikolaei, K. Hosseinzadeh, M. Yassari, H. Sadeghi, D. D. Ganji, Analytical and numerical solution of non-Newtonian second-grade fluid flow on a stretching sheet, *Therm. Sci. Eng. Prog.*, 5 (2018) 309–316.
- [11] F. Salah, M. H. Elhafian, Numerical solution for heat transfer of non-newtonian second-grade fluid flow over stretching sheet via successive linearization method, *IAENG Int. J. Appl. Math.*, 49 (2019) 1–8.
- [12] D. Dey, Non-Newtonian Effects on Hydromagnetic Dusty Stratified Fluid Flow Through a Porous Medium with Volume Fraction, *Proc. Natl. Acad. Sci. India Sect. A - Phys. Sci.*, 86 (2016) 47–56.
- [13] D. Dey, Hydromagnetic Oldroyd fluid flow past a flat surface with density and electrical conductivity stratification, *Lat. Am. Appl. Res.*, 42 (2017) 41–45.
- [14] B. ShankarGoud, Thermal Radiation Influences on MHD Stagnation Point Stream over a Stretching Sheet with Slip Boundary Conditions, *Int. J. Thermofluid Sci. Technol.*, 7 (2020)

- 1–11.
- [15] T. Hayat, S. Qayyum, S. Ali Shehzad, A. Alsaedi, MHD nonlinear convective flow of oldroyd-b fluid in a darcy-forchheimer porous medium with heat generation/absorption, *J. Porous Media*, 21 (2018) 389–404.
- [16] B. Sailaja, G. Srinivas, B. S. Babu, Free and Forced Convective Heat Transfer through a Nanofluid with Two Dimensions past Stretching Vertical Plate, *Int. J. Thermofluid Sci. Technol.*, 7 (2020).
- [17] J. H. Merkin, On dual solutions occurring in mixed convection in a porous medium, *J. Eng. Math.*, 20 (1986) 171–179.
- [18] M. Turkyilmazoglu, Multiple analytic solutions of heat and mass transfer of magnetohydrodynamic slip flow for two types of viscoelastic fluids over a stretching surface, *J. Heat Transfer*, 134 (2012) 1–9.
- [19] K. Zaimi, A. Ishak, Boundary Layer Flow and Heat Transfer over a Permeable Stretching/Shrinking Sheet with a Convective Boundary Condition, *J. Appl. Fluid Mech.*, 8 (2015) 499–505.
- [20] Naramgari, Sandeep, C. Sulochana, Dual solutions for MHD stagnation-point flow of a nanofluid over a stretching surface with induced magnetic field, *Int. J. Sci. Eng.*, 9 (2015) 1–8.
- [21] N.S. Anuar, N. Bachok, N.M. Arifin, H. Rosali, Effect of Suction/Injection on Stagnation Point Flow of Hybrid Nanofluid over an Exponentially Shrinking Sheet with Stability Analysis, *CFD Lett.*, 11 (2019) 21–33.
- [22] D. Dey, R. Borah, Dual Solutions of Boundary Layer Flow with Heat and Mass Transfers over an Exponentially Shrinking Cylinder: Stability Analysis, *Lat. Am. Appl. Res.*, 50 (2020) 247–253.
- [23] S. D. Harris, D. B. Ingham, I. Pop, Mixed convection boundary-layer flow near the stagnation point on a vertical surface in a porous medium: Brinkman model with slip, *Transp. Porous Media*, 77 (2009) 267–285.
- [24] D. Dey, M. Hazarika, Entropy Generation of Hydro-Magnetic Stagnation Point Flow of Micropolar Fluid With Energy Transfer Under the Effect of Uniform Suction / Injection, *Latin American Applied Research*, 50 (2020) 209–214.
- [25] D. Dey, B. Chutia, Dusty nanofluid flow with bioconvection past a vertical stretching surface, *J. King Saud Univ. - Eng. Sci.*, (2020).